Pergamon

Scripta Materialia, Vol. 36, No. 8, pp. 867-874, 1997
Elsevier Science Ltd

1359-6462/97 $17.00 +.00

PII S1359-6462(96)00499-X

AN ANALYTICAL MODEL FOR PERITECTIC TRANSFORMATION WITH EXPERIMENTAL VERIFICATION

A. Das, I. Manna and S. K. Pabi
Department of Metallurgical and Materials Engineering
Indian Institute of Technology, Kharagpur 721 302, India.

(Received May 24, 1996)
(Accepted October 7,1996)

Introduction

Formation of a new solid phase on cooling a binary two phase aggregate comprising a solid and liquid is termed as peritectic transformation [1]. Except for the grain refinement of a few Al-based alloys [2–6], the technological application of peritectic transformation has so far been limited. However, the recent method of synthesizing the superconducting YBCO-compounds through peritectic transformation necessitates a better understanding of the mechanism and kinetics of this liquid → solid transformation [7–12]. Experimental studies on peritectic transformation are often jeopardized by its relatively complex transformation mechanism, extremely slow reaction kinetics, and presence of a liquid phase in the microstructure during the phase transition. Besides, distinction between the peritectic transformation product (or secondary phase) and directly solidified remnant liquid in the microstructure is often too difficult. As a result, the experimental data on peritectic transformation kinetics are scarcely available. As an alternative, several attempts have been made in the past to formulate mathematical models on peritectic transformation. For instance, Titchner and Spittle [13] have proposed that the secondary phase thickness (w) varies with time (t) through a power law: $w = At^n$, where A is a constant and n is the time exponent varying between 0.36–0.57 depending on the concerned alloy system. St. John and Hogan [14] have utilized the Wagner equation [15] for diffusion controlled growth of an intermediate phase to arrive at a similar power law with $n = 0.5$. Maxwell and Hellawell [5] have proposed a model, assuming a Laplacian concentration profile in the product phase that restricts the solution only to the dilute alloys. Recently, Lopez [16] has considered a quasi-static interface diffusion across the product phase and a stationary profile in cored or homogeneous primary phase to derive an analytical expression for peritectic growth. It is apparent that these models embrace several oversimplified assumptions and lack in systematic validation with the relevant experimental data. In this paper, a simple mathematical model on the kinetics of peritectic transformation has been proposed and its predictions have been compared with the experimentally determined data from the Cd-Ag system. It may be noted that the kinetic data on isothermal peritectic transformation in the Cd-Ag system, which yields excellent microstructures for kinetic analysis, have not been reported earlier.

The Mathematical Model

Fig. 1 presents a schematic binary phase diagram where the two phase mixture comprising the pro-peritectic solid (β) of composition $C_{\beta p}$ and liquid (L) of composition C_{lp} undergoes peritectic transformation to form the α-phase on cooling through the peritectic temperature (T_p) as follows: $\beta + L \rightarrow \alpha$. If the β particles are assumed to be equispaced spheres of uniform size, the phase transformation kinetics in the alloy can be represented by the rate of transformation in a cell of radius, $R_i = [N_\beta(3/4\pi)]^{1/3}$, where N_β is the number of β nuclei per unit volume (Fig. 2). Continuous cooling of an alloy of composition C_0 from the liquid state to T_p results into a transformation cell comprising β of radius S_{1p} inside a liquid pool of outer radius R_i. If the slow cooling continues up to a temperature T_1 ($< T_p$), a very thin layer of α of thickness (S_{2p} -S_{1p}) would form around β. Here the growth of α is accompanied by the migration of both α-β interface located at S_1 and α-liquid interface at S_2 during the isothermal peritectic transformation at T_1. It may be noted that the mass transport in peritectic transformation has several similarities with that in precipitate dissolution. It is known that the linearized composition gradient approximation [17] yields a much better estimate of the dissolution kinetics as compared to that assuming an invariant interface location [18]. Hence, the concentration gradient in α enveloped between two moving interfaces in diffusion controlled peritectic transformation at the temperature T_1 (Fig. 1) has been assumed to be linear in the spatial variable (r) as shown in Fig. 2(b).

S_{1p} at T_p may be obtained from the overall mass balance within the transformation cell as:

$$(4/3)\pi(S_{1p})^3 C_{\beta p} + (4/3)\pi(R_i^3 - S_{1p}^3)C_{lp} = (4/3)\pi R_i^3 C_0$$

or,

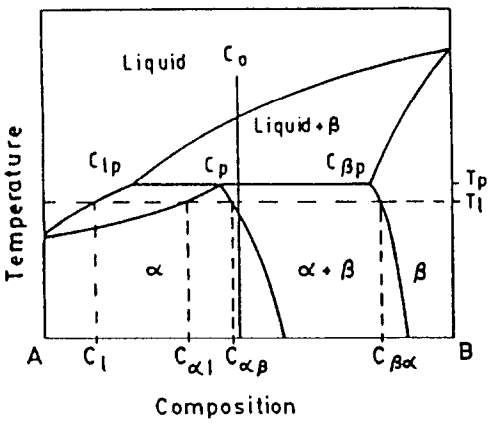

Figure 1. A schematic binary phase diagram defining the concentration terms in peritectic transformation.

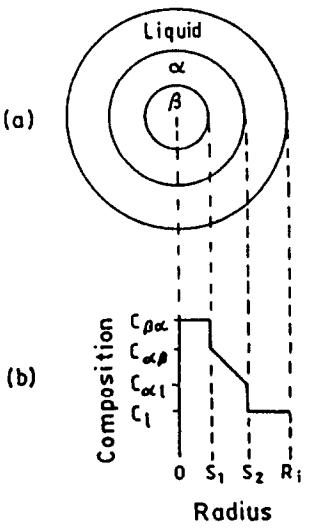

Figure 2. (a) A transformation cell and (b) the schematic composition-distance profiles in it, during peritectic transformation in an alloy of composition C_0 at T_1 of Fig. 1.

$$S_{1p} = R_i\{(C_0 - C_{lp})/(C_{\beta p} - C_{lp})\}^{1/3} \quad (1)$$

where $C_{\beta p}$ and C_{lp} represent the respective concentration values of the β and liquid phases in contact with each other.

Applying Zener's linearized concentration gradient approach [17] to the α phase, S_{2p} at the onset (i.e. t = 0) of isothermal transformation at T_1 may be determined through a similar exercise:

$$\frac{4}{3}\pi S_{1p}^3 C_{\beta\alpha} + \frac{4}{3}\pi(S_{2p}^3 - S_{1p}^3)\frac{1}{2}(C_{\alpha\beta} + C_{\alpha 1}) + \frac{4}{3}\pi(R_i^3 - S_{2p}^3)C_1 = \frac{4}{3}\pi R_i^3 C_0$$

or,

$$S_{2p} = \left[\frac{R_i^3(C_0 - C_1) + S_{1p}^3\left\{\frac{1}{2}(C_{\alpha\beta} + C_{\alpha 1}) - C_{\beta\alpha}\right\}}{\frac{1}{2}(C_{\alpha\beta} + C_{\alpha 1}) - C_1}\right]^{\frac{1}{3}} \quad (2)$$

where, $C_{\alpha\beta}$ and $C_{\alpha l}$ are the α–compositions (at T_1) at the α–β and the α-liquid interfaces, respectively. Here, the mixing in the liquid at T_1 is considered to be fast enough to make it homogeneous with composition C_l, while, composition in β is assumed to be constant at $C_{\beta\alpha}$. From the mass balance condition, the location of the α-liquid interface (S_2) at a given t may be determined as follows:

$$S_2 = \left(\frac{AR_i^3 + BS_1^3}{K}\right)^{1/3} \quad (3)$$

where $A = (C_0 - C_l)$, $B = [\{0.5\,(C_{\alpha\beta} + C_{\alpha l})\} - C_{\beta\alpha}]$, and $K = [\{0.5\,(C_{\alpha\beta} + C_{\alpha l})\} - C_l]$. Similarly, the β–α interface location at a given t can be obtained from the mass balance condition across that interface:

$$(C_{\beta\alpha} - C_{\alpha\beta})\frac{dS_1}{dt} = D_\alpha\left[\frac{dC}{dr}\right]_{r=S_1} = D_\alpha\left(\frac{C_{\alpha 1} - C_{\alpha\beta}}{S_2 - S_1}\right) \quad (4)$$

where D_α is the volume diffusion coefficient in α. Substituting S_2 from equation (3) in equation (4) and rearranging, it may be readily shown that,

$$\int_{S_{1p}}^{S_1}\left[\left(\frac{AR_i^3 + BS_1^3}{K}\right)^{1/3} - S_1\right]dS_1 = D_\alpha\left(\frac{C_{\alpha 1} - C_{\alpha\beta}}{C_{\beta\alpha} - C_{\alpha\beta}}\right)\int_0^t dt. \quad (5)$$

The left hand side of in equation (5) can be further simplified, since,

$$\left(\frac{AR_i^3 + BS_1^3}{K}\right)^{1/3} = \left(\frac{A}{K}\right)^{1/3} R_i\left[1 + \frac{B}{A}\left(\frac{S_1}{R_i}\right)^3\right]^{1/3}. \quad (6)$$

For $\{(B/A)(S_1/R_i)^3\} << 1$, binomial expansion of the term in square bracket in equation (6) followed by truncation of $(S1/R_i)^9$ and higher order terms, yields:

$$\left(\frac{AR_i^3 + BS_1^3}{K}\right)^{1/3} = R_i\left(\frac{A}{K}\right)^{1/3}\left[1 + \frac{1}{3}\left(\frac{B}{A}\right)\left(\frac{S_1}{R_i}\right)^3 - \frac{1}{9}\left(\frac{B}{A}\right)^2\left(\frac{S_1}{R_i}\right)^6\right]. \quad (7)$$

Substitution of equation (7) in equation (5) results in the expression:

$$\left[S_1+\frac{1}{12}\left(\frac{B}{A}\right)\left(\frac{S_1^4}{R_i^3}\right)-\frac{1}{63}\left(\frac{B}{A}\right)^2\left(\frac{S_1^7}{R_i^6}\right)-\frac{S_1^2}{2}\left(\frac{K}{A}\right)^{1/3}\frac{1}{R_i}\right]_{S_{1_p}}^{S_1}=\frac{D_\alpha}{R_i}\left(\frac{K}{A}\right)^{1/3}\left(\frac{C_{\alpha 1}-C_{\alpha\beta}}{C_{\beta\alpha}-C_{\alpha\beta}}\right)t$$

or,

$$S_1-a_1S_1^2+a_2S_1^4-a_3S_1^7-b=\frac{D_\alpha}{R_i}\Phi t \tag{8}$$

where,

$$a_1=\frac{1}{2R_i}\left(\frac{K}{A}\right)^{1/3},\quad a_2=\frac{1}{12R_i^3}\left(\frac{B}{A}\right),\quad a_3=\frac{1}{63R_i^6}\left(\frac{B}{A}\right)^2,\quad \Phi=\left(\frac{C_{\alpha 1}-C_{\alpha\beta}}{C_{\beta\alpha}-C_{\alpha\beta}}\right)\left(\frac{K}{A}\right)^{1/3}.$$

At t = 0, equation (8) reduces to:

$$b=S_{1_p}-a_1S_{1_p}^2+a_2S_{1_p}^4-a_3S_{1_p}^7 \tag{9}$$

Equation (8), may now be used (incorporating the values of the constants a_1, a_2, a_3, b and Φ) to readily determine the β–α interface position at any given t during the isothermal peritectic transformation. Subsequently, the α-liquid interface position (S_2) at that instant is obtained by substituting the value of S_1 in equation (3).

Experimental

Two Cd-rich binary alloys containing 4 and 5 at.% Ag were prepared by melting high purity (> 99.99 wt.%) Cd and Ag in evacuated and argon filled glass capsules. The molten alloys were furnace cooled to $T_1 < T_p$ (= 616 K) and quenched in iced brine to room temperature to retain the microstructure at T_1. Subsequent isothermal kinetic studies at T_1, (controlled to ±1 K) were carried out by reheating cylindrical samples of 3 mm diameter, cut from the quenched ingot and encapsulated in evacuated glass tubes (with 3 mm inner diameter) to prevent oxidation and minimize gravity segregation. Following the isothermal treatments for varying lengths of t, the samples were quenched in iced brine and subjected to an extensive microstructural investigation under the optical microscope. The polished samples were etched with a solution containing 40 g of CrO_3 and 3 g of Na_2SO_4 in 200 ml distilled water. The area fraction of β was estimated through the 'systematic point count method' [19] using a 25 × 25 square grid eyepiece at 100X magnification.

Results and Discussions

The Cd-Ag system is considered suitable for validation of the present model because peritectic transformation in Cd-Ag occurs at a relatively lower temperature (T_p = 616 K) and is not succeeded by any other phase transition that could change the microstructure. Furthermore, α in this system is known to form predominantly by the peritectic transformation instead of a direct/isomorphous solidification from the remnant liquid [14]. It may be pointed out that the microstructure following peritectic transformation in Cd-Ag is far more revealing for kinetic analysis than those in other systems like Pb-Bi reported in the literature [20].

Fig. 3 presents a typical microstructure comprising the bright dendrites of β surrounded by a thin but uniform layer of α (dark), developed in the course of continuous cooling from the liquid state to T_1 = 603 K (< T_p) followed by quenching in iced brine to reveal the microstructure at the onset (i.e. t = 0) of peritectic transformation. Here the remnant liquid has solidified into a very fine two phase (α + β) aggregate (Fig. 3). Following reheating to T_1, the thickness of the α layer now increases with t during isothermal holding at T_1 due to peritectic transformation. For instance, the α-envelope formed at T_1 after t = 15 min (Fig. 4) is thicker than that at t = 0 (Fig. 3). It is evident that the area fraction of α in the microstructure increases with t at a given T_1 at the expense of both β and liquid. However, the rate of consumption of liquid is faster than that for dissolution of β, since the net solute flux across the liquid-α interface is possibly more than the same across the β-α boundary. Fig. 5 reveals that the volume fraction of α ≈ 0.6 after isothermal treatment at T_1 for 2 h, as compared to that of 0.05–0.1 in the as-quenched condition (Fig. 3). Similarly, the volume fraction of β in Fig. 5 is less than 0.4 of that in Fig. 3. Microstructural features typical to the later stage of peritectic transformation is illustrated in Fig. 6. Here the area 'A' represents a typical cavity formed due to the expulsion of liquid which could otherwise solidify into a fine two phase structure (like in area 'C') following quenching from T_1. Therefore, it appears that the microstructure only in the early part of the transformation (say, in Figs. 3 and 4) conforms reasonably to the idealized configuration of the transformation cells in Fig. 2. The microstructural features observed in Cd-5 at.% Ag alloy are quite similar to those in Cd-4 at.% Ag alloy.

Figs. 7 and 8 compare the predictions of the present model with the experimental data from the Cd-4 and 5 at.% Ag alloys, respectively. Input parameters used for the calculations are presented in Table 1. It is evident that the predicted transformation kinetics are in excellent agreement with the experimentally measured data until $D_\alpha t/R_i^2 = 0.5$. Beyond this point, the predicted rates appear to be significantly faster than the experimental data, possibly due to the experimental uncertainties. For instance, the idealized geometry of the transformation cell (Fig. 2) may not be tenable at $D_\alpha t/R_i^2 > 0.5$ as: (a) the liquid pool ceases to be interconnected, and (b) the displacement of the entrapped liquid leads to the formation of voids (e.g. region 'A' in Fig. 6). As a result, the transformation kinetics can slow down significantly, resulting in the divergence between the predicted results and experimental data beyond $D_\alpha t/R_i^2 > 0.5$ (cf. Figs. 7 and 8). Nevertheless, the observed trend of gradual retardation of the transformation kinetics is qualitatively corroborated by the results predicted by the present model.

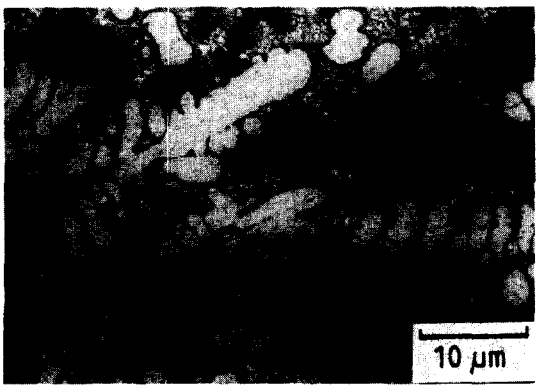

Figure 3. Microstructure of the Cd-4at.% Ag alloy, furnace cooled to 603 K from the liquid state and quenched in iced brine.

Figure 4. Microstructure of the Cd-4at.% Ag alloy, quenched in iced brine after isothermal holding for 15 minutes at 603 K.

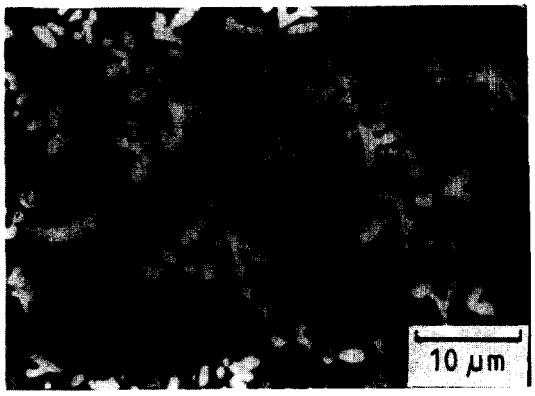

Figure 5. Quenched microstructure of a Cu-4at.% Ag alloy, following isothermal transformation at 603 K for 2 h.

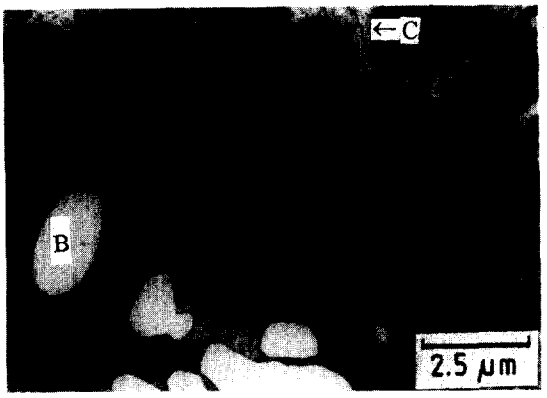

Figure 6. A magnified view of Fig. 5, illustrating the β (area marked 'B'), α (dark grey) and liquid (marked 'C') at a later stage of isothermal peritectic transformation (2 h) at 603 K. Dark area (marked 'A') in the microstructure represent a cavity formed due to expulsion of the liquid.

Until now, the most detailed analysis of peritectic transformation kinetics has been carried out by Lopez [16] considering either a cored or constant composition profile in β within a finite geometry of the transformation cell. The results from this model have, however, not been validated by a suitable comparison with the experimental data. Figs. 7 and 8 show the kinetics predicted by the Lopez model for the present alloys. When the β composition is assumed constant, Lopez analysis shows a poor agreement with the experimental data at $D_\alpha t/R_i^2 > 0.2$, possibly due to the quasi-static interface approximation in this model. In fact, it has earlier been shown that the interfacial movement in a moving

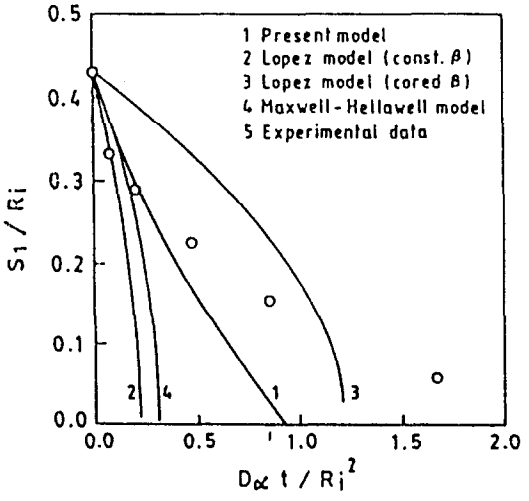

Figure 7. Variation of normalized β radius (S_1/R_i) versus normalized time ($D_\alpha t/R_i^2$) for peritectic transformation in a Cd-4at.% Ag alloy. Experimental data are represented by open circles.

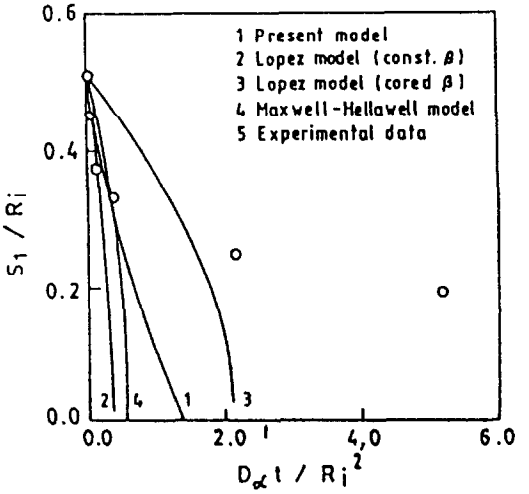

Figure 8. Peritectic transformation kinetics in a Cd-5at.% Ag alloy. Experimental data are represented by open circles.

TABLE 1
Input Parameters for the Calculation of Peritectic Transformation Kinetics in Cd-Ag System.

C_0	T_I	Equilibrium Compositions (at.%)						R_i	D_α
(at.%)	(K)	$C_{\beta p}$	C_{lp}	$C_{\beta\alpha}$	$C_{\alpha\beta}$	$C_{\alpha l}$	C_l	(m)	(m^2/sec)
Cd-4Ag	603	80.75	97.4	80.75	93.1	96.9	98.8	1.2×10^{-4}	1×10^{-12}
Cd-5Ag	608	80.75	97.4	80.75	93.0	96.0	98.4	1.2×10^{-4}	1×10^{-12}

boundary problem like precipitate dissolution [18] influences the local concentration gradients at the interface, and consequently, has a significant influence in the mass balance across the interface. When the Lopez model assumes a cored composition profile in β, the predicted results deviate significantly from the experimental data throughout the transformation. Here, the divergence appears to originate from the quasi-static interface approximation, as well as, time invariant cored composition profile in β. On the other hand, Figs. 7 and 8 show that the Laplacian concentration profile assumed in Maxwell and Hellawell model [5] yields a satisfactory agreement with the experimental data only during the early stage of transformation ($D_\alpha t/R_i^2 < 0.25$), when the effect of impingement of the diffusion fields can be ignored. In summary, the results predicted by the present model seem to be closer to the experimental data than those obtained from other models proposed earlier [5,16].

Conclusion

An analytical model on the kinetics of peritectic transformation based on the linearized concentration gradient approximation has been presented and validated through a suitable comparison with the relevant experimental data from the Cd-Ag system. The predictions by the present model show a better agreement with the experimental results than those by the earlier proposed models. The observed reaction rates, however, show divergence from the rates computed through the present model at the later stages of transformation ($D_\alpha t/R_i^2 > 0.5$) possibly due to the deviation from the idealized geometry arising out of liquid entrapment and/or void formation.

References

1. A. D. Pelton, in: Phase Transformations in Materials, Materials Science and Technology, R.W. Cahn, P. Haasen and E.J. Kramer (Eds.), **vol.5**, p.29, VCH Verlagsgesellschaft GmbH, Weinheim, FRG (1991).
2. F.A. Crosley and L.F. Mondolfo, Trans. AIME **191**, 1143 (1951).
3. A. Cibula, J. Inst. Metals **76**, 321 (1949).
4. I. Maxwell and A. Hellawell, Trans. AIME **3**, 1487 (1972).
5. I. Maxwell and A. Hellawell, Acta Metall. **23**, 901 (1975).
6. P.C. VanWiggen and W.H.M. Alsem, Light Metals, p.763, Proc. TMS Annual Meeting Warrendale, Pennsylvania (1993).
7. K. Sawano, M. Morita, K. Miyamoto, K. Doi, A. Hayashi and M. Murakami, J. Ceramic Soc. Japan **97**, 1028 (1989).
8. A. Goyal, P.D. Funkenbusch, D.M. Kroger and S.J. Burns, Physica C: Superconductivity **182**, 203 (1991).
9. Y.A. Jee, S.J.L. Kang, J.H. Suh and D.Y. Yoon, J. Amer. Ceramic Soc. **76**, 2701 (1993).
10. N. Pellerin, P. Odier, P. Simon and D. Chateigner, Physica C: Superconductivity **228**, 351 (1994).
11. C.J. Kim, K.B. Kim and G.W. Hong, Materials Letters **21**, 9 (1994).
12. M. Ullrich and H.C. Freyhardt, Physica C: Superconductivity **235–240**, 455 (1994).
13. A.P. Titchner and J. A. Spittle, Metal Sci. **8**, 112 (1974).
14. D.H. St. John and L.M. Hogan, Acta Metall. **25**, 77 (1977).
15. C. Wagner, Acta Metall. **17**, 99 (1969).

16. H. F. Lopez, Acta Metall. Mater. **39**, 1543 (1991).
17. C. Zener, J. Appl. Phys. **20**, 962 (1947).
18. S. K. Pabi, Acta Metall. **27**, 1693 (1979).
19. J. E. Hilliard in : Quantitative Microscopy, R. T. DeHoff and F. N. Rhines (Eds.), p.52, McGraw-Hill Book Company, New York (1968).
20. D. M. Goddard and W. J. Childs, J. Less Common Metals **58**, 217 (1978).